Available online at www.sciencedirect.com
ScienceDirect
Journal of Organometallic Chemistry 693 (2008) 1117–1126
Journal of Organometallic Chemistry
www.elsevier.com/locate/jorganchem

Synthesis, characterization, *in vitro* cytotoxicity and anti-inflammatory activity of palladium(II) complexes with tertiary phosphines and heterocyclic thiolates: Crystal structure of $[PdC_{28}H_{19}N_8PS_2]$

Farkhanda Shaheen [a,*], Amin Badshah [a], Marcel Gielen [b,*], Christine Gieck [c], Mariyam Jamil [d], Dick de Vos [e]

[a] *Department of Chemistry, Quaid-i-Azam University, Islamabad 45320, Pakistan*
[b] *Vrije Universiteit Brussel, Faculty of Engineering, HNMR Unit, B-1050 Brussels, Belgium*
[c] *Università del Piemonte Orientale, 15100 Alessandria, Italy*
[d] *Department of Biology, Faculty of Biological Science, Quaid-I-Azam University, Islamabad 45320, Pakistan*
[e] *Pharmachemie BV, PO Box 552, 2003 RN Haarlem, The Netherlands*

Received 12 August 2007; received in revised form 6 January 2008; accepted 6 January 2008
Available online 11 January 2008

Abstract

The new four-coordinated mononuclear palladium(II) complexes **1**–**9** with chelating heterocyclic thiolates and tertiary phosphines with general formula $[Pd(L)_nCl(R'R_2P)]$ (L = Pym2SH (pyrimidine-2-thiolate), Pur6SH (purine-6-thiolate), Py2SH (pyridine-2-thiolate), $R_3P = PPh_3$, P(*o*-tolyl)$_3$, PPh_2Cl), $n = 1, 2$) have been synthesized by the direct reaction of $[PdCl_2(R'R_2P)_2]$ with polyfunctional heterocyclic thiolates which display a wide variety of coordinations. These compounds were characterized by elemental analysis, FT-IR and multinuclear (^1H, ^{13}C and ^{31}P) NMR. The X-ray diffraction study of non-ionic compound **5** showed that the thiolate acts as unidentate and that the chelating (–N,S) ligand adopts a slightly distorted square planar geometry around the palladium atom. *In vitro* the anti-inflammatory inhibition of compounds **1**–**9** was 10–15% greater than that of the standard drug Declofenac. Compounds **1** and **4** showed mostly a moderate to low cytotoxicity against seven human tumor cell lines whereas compound **3** was somewhat more active.

Keywords: Thiolate; Palladium; Anti-inflammatory activity; Cytotoxity

1. Introduction

In the last several decades, the chemistry of palladium(II) complexes containing heterocyclic thiolate ligands has received considerable attention due to their wide-range of applications such as fungicide [1,2], in the pharmaceutical industry [3] and as electrical conductors [4]. For catalytic applications, the co-ordination chemistry of heterocyclic thiolates and their corresponding anions as ligands is very rich, combining S and N ends [5] and mimicking the electronic and structural properties of the active sites of metallo-enzymes [6]. Palladium thiolates have significant applications in biological systems due to the palladium–sulfur interaction [7]. In some cases, the metal complexes of these bases, especially those of Pt(II) and Pd(II), show a higher anticancer activity than the free ligands [8]. On the other hand, phosphines and phosphine metal containing complexes have been actively studied due to their extensive uses as antitumor and anti-inflammatory

* Corresponding authors. Tel.: +32 2 629 32 79; fax: +32 2 629 32 81 (M. Gielen).
E-mail addresses: fshaheenpk@yahoo.com (F. Shaheen), mgielen@vub.ac.be (M. Gielen).

0022-328X/$ - see front matter © 2008 Elsevier B.V. All rights reserved.
doi:10.1016/j.jorganchem.2008.01.005

drugs [9]. Heterocyclic thiolates ligands contain at least one deprotonated heterocyclic thioamid group $(N–C–S)^-$ and can act not only as monodentate, involving either the exocyclic sulfur (η^1-S) [10] or the endocyclic nitrogen (η^1-N) [11] but also as chelating and bridging ligands [12]. Purine-6-thiolate (Pur6SH) has attracted some attention because of its multiple and versatile binding sites such as N^1, N^3, N^7, N^9, S^6, while from the N,S-chelating site, two nitrogen atoms (N^1 and N^7) can compete to be involved in co-ordination to the central palladium atom. The final structure depends on the stability of N^1/S^6 or N^7/S^6 end of the formed square planar structure. With pyridine-2-thiolate (Py2SH) and pyrimidine-2-thiolate (Pym2SH), coordination can occur through the S and N,S-chelating sites. In our previous work, we have studied the coordination behavior of heterocyclic thiolates with palladium (II) [13]. As a continuation of our studies on versatile coordination modes, effective biological activities and in connection with the current interest in the coordination chemistry of palladium(II) compounds with heterocyclic thiolates, we selected three interesting ligands: derivatives of pyrimidine, purine and pyridine: pyrimidine-2-thiolate (Pym2SH), purine-6-thiolate (Pur6SH) and pyridine-2-thiolate (Py2SH) of which a series of palladium(II) complexes were synthesized.

2. Experimental

2.1. Reagents

Pyrimidine-2-thione, purine-6-thione, pyridine-2-thione, triphenylphosphine, tris-*o*-tolylphosphine, chlorodiphenylphosphine and palladium(II) chloride were of analytical grade and were purchased from Aldrich (USA). All the organic solvents were dried before use according to standard procedures [14].

2.2. Instrumentation

Elemental analyses were carried out on a Fisons EA1108 CHNS-O microanalyser. FT-IR spectra were recorded on a Bio-Rad Excalibur apparatus FT-IR, model FTS 3000 MX using KBr discs from 4000 to 400 cm^{-1} and CsI discs from 500 to 200 cm^{-1} with a Perkin–Elmer FT-IR Nexus spectrometer.

The ^1H and ^{13}C NMR spectra were recorded in DMSO-d_6 solutions on a Bruker 300 MHz spectrometer operating at 300 and 75.5 MHz, respectively. The ^{31}P NMR spectra were recorded in $CDCl_3$ solutions on a Bruker AMX-400 MHz spectrometer operating at 160 MHz.

Single crystal X-ray diffraction data of **5** was collected at 293 K using an Oxford Diffraction Xcalibur 2 diffractometer with Mo Kα radiation. Data reduction and analytical absorption correction were performed using the CRYSALIS RED software suite [15]. The structure was solved using SIR2004 [16] and refined using SHELXL97 [17].

2.3. Synthesis (see Scheme 1)

2.3.1. Synthesis of the precursor $[Pd(PR_2R')Cl_2]$

The precursor $[Pd(PR_2R')_2Cl_2]$, where R = phenyl, *o*-tolyl and R′ = phenyl, *o*-tolyl and chloro, respectively, were synthesized according to literature methods [14,15,20] by the reaction of palladium(II) chloride in 25 cm^3 of ethanol with a few drops of 1 N hydrochloric acid and PR_2R' in 25 cm^3 acetone ($PdCl_2$:PR_2R' = 1:2). The reaction mixture was refluxed for 2 h to yield a pale-yellow precipitate that was washed with an excess of ethanol, dried in air and recrystallized from THF, to yield light yellow crystals after 48 h.

2.3.2. Synthesis of chloro-(pyrimidine-2-thiolato)(triphenylphosphine)palladium(II) (**1**)

The ligand Pym2SH (0.039 g, 0.34 mmol) was mixed with a suspension of $PdCl_2(PPh_3)_2$ (0.15 g, 0.34 mmol) (1:1 molar ratio) in 25 cm^3 of CH_2Cl_2. The reaction mixture was refluxed for an hour to yield a clear solution. The solvent was evaporated under reduced pressure. The solid product was recrystallized from a mixture of CH_2Cl_2 and *n*-hexane (3:1 molar ratio). (Yield: 85%). Anal. Calc. for $C_{22}H_{18}ClN_2PPdS$ calc (obs): C, 51.28 (51.23); H, 3.52 (3.46); N, 5.44 (5.45); S, 6.22 (6.24). FT-IR: 1595, *ν*(C=N), 340, *ν*(Pd–S), 443, *ν*(Pd ← N), 289, *ν*(Pd–Cl) cm^{-1}; ^1H NMR (DMSO-d_6): 6.98 (d, $^3J_{HH}$ = 6.5 Hz, H(4)) ppm, 8.23 (d, $^3J_{HH}$ = 7.3 Hz, H(6)) ppm, 6.46 (m, 1H(5)) ppm, 7.2-7.6 (m, 15H, Ph-H) ppm. ^{13}C NMR (DMSO-d_6): 187.25(C2), 158.91(C4), 109.2(C5), 162.34 (C6); $^{31}P\{^1H\}$ NMR ($CDCl_3$): *δ* 31.5 (s, PPh_3).

2.3.3. Synthesis of chloro-(pyrimidine-2-thiolato)-(tris-o-tolylphosphino)palladium(II) (**2**)

(Yield: 85%). Anal. Calc. for $C_{25}H_{24}ClN_2PPdS$ calc (obs): C, 53.87 (53.83); H, 4.34 (4.32); N, 5.02 (5.01); S, 5.75 (5.72). FT-IR: 1598, *ν*(C=N), 329, *ν*(Pd–S), 440, *ν*(Pd ← N), 301, *ν*(Pd–S) cm^{-1}; ^1H NMR (DMSO-d_6): 8.29 (d, $^3J_{HH}$ = 6.9 Hz, 2H(4 or 6)) ppm, 8.34 (d, $^3J_{HH}$ = 7.3 Hz, 2H(4 or 6)) ppm, 6.95 (m, 1H(5)) ppm, 7.2–7.5 (m, 12H, tolyl-H) ppm; 1.9–2.3 (m, 9H, –CH_3) ppm; ^{13}C NMR (DMSO-d_6): 177.35 (C2), 156.23 (C4), 106.99 (C5), 161.24 (C6), $^{31}P\{^1H\}$ NMR ($CDCl_3$): *δ* 32.85, (s, P(*o*-Tol)$_3$).

2.3.4. Synthesis of chloro-(pyrimidine-2-thiolato)(chlorodiphenylphosphine)palladium(II) (**3**)

Pyrimidine-2-thione (0.039 g, 0.34 mmol) was mixed with a suspension of $PdCl_2(ClPh_2P)_2$ (0.15 g, 0.34 mmol) in 20 cm^3 of CH_2Cl_2 (1:1 molar ratio). The reaction mixture was refluxed for half an hour to obtain a clear solution. The obtained product was recrystallized from CH_2Cl_2/*n*-hexane by a slow evaporation at room temperature. (Yield: 83%). Anal. Calc. for $C_{16}H_{13}Cl_2N_2PPdS$ calc (obs): C, 40.57 (40.63); H, 2.77 (2.73); N, 5.91 (5.91); S, 6.77(6.76). FT-IR: 1592, *ν*(C=N), 339, *ν*(Pd–S), 423, *ν*(Pd ← N), 296, *ν*(Pd–Cl) cm^{-1}; ^1H NMR (DMSO-d_6):

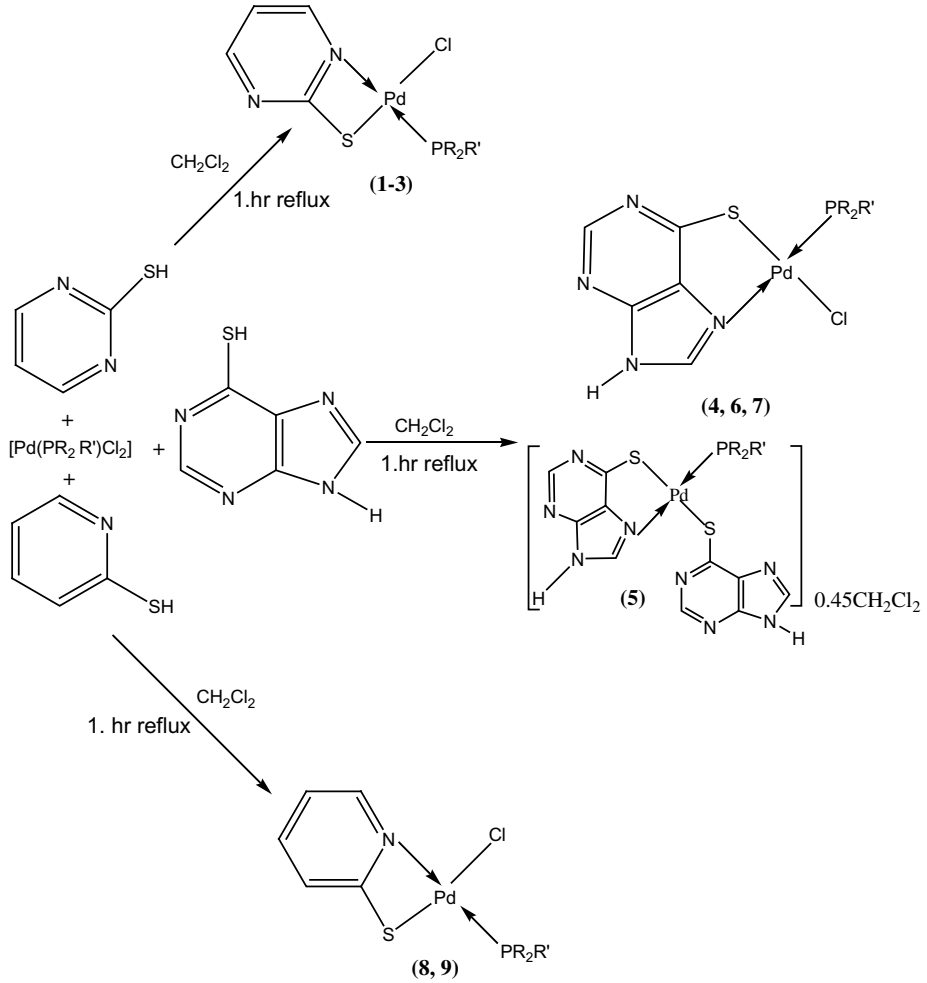

R= phenyl, o-tolyl, R' = phenyl,o-tolyl for(1, 2, 4, 5, 6, 8, 9), Chloro for (3, 7)

Scheme 1. Synthetic scheme for compounds **1–9**.

8.27 (d, $^3J_{HH} = 8.2$ Hz 2H(4 or 6)) ppm, 8.25 (d, $^3J_{HH} = 8.29$ Hz, 2H(4 or 6)) ppm, 6.82 (m, 1H(5)) ppm, 7.4–7.8 (m, 10H, Ph-H) ppm; ^{13}C NMR (DMSO-d_6): 179.3 (C2), 151.2 (C4), 106.5 (C5), 168.54 (C6), ^{31}P{^{1}H} NMR ($CDCl_3$): δ 30.6 (s, $ClPh_2P$).

2.3.5. Synthesis of chloro-(purine-6-thiolato)(triphenylphosphino)palladium(II) (**4**)

(Yield: 87%). Anal. Calcd. for $C_{23}H_{18}ClN_4PPdS$ calcd (obs): C, 49.74 (49.79); H, 3.26 (3.22); N, 10.08 (10.04); S, 5.75 (5.77). FT-IR: 1590–1640, ν(C=N), 305, ν(Pd–Cl), 405, ν(Pd–S), 399, ν(Pd ← N) cm^{-1}; ^{1}H NMR (DMSO-d_6): 6.92 (d, $^3J_{HH} = 7.9$ Hz, 1H(8)) ppm, 7.85 (d, $^3J_{HH} = 8.0$ Hz, 1H(9)) ppm, 8.93 (s, 1H(2)) ppm, 7.4–7.6 (m, 15H, Ph-H) ppm; ^{13}C NMR (DMSO-d_6): 192.3 (C2), 182.5 (C4), 181.9 (C5), 187.5 (C6), 172.5 (C8), ^{31}P{^{1}H} NMR ($CDCl_3$): δ 31.7 (s, PPh_3).

2.3.6. Synthesis of bis-(purine-6-thiolato)(triphenylphosphine)palladium(II)dichloride (**5**)

A suitable crystal for X-ray diffraction was obtained by dissolving 0.5 g of the sample in a small quantity of CH_2Cl_2 and *n*-hexane (3:1). A slow evaporation at room temperature for several days resulted in small orange crystals (Yield: 85%). Anal. Calc. for $C_{28}H_{21}N_8PPdS_2$ [0.45 CH_2Cl_2] calcd (obs): C, 43.11 (43.09); H, 2.71 (2.71); N, 14.39 (14.40); S, 8.22 (8.25). FT-IR: 1598–1640, ν(C=N), 415, ν(Pd–S), 397, ν(Pd ← N) cm^{-1}; ^{1}H NMR (DMSO-d_6): 6.88 (d, $^3J_{HH} = 7.0$ Hz, 1H(8)) ppm, 7.23 (d, $^3J_{HH} = 7.0$ Hz, 1H, NH(9)) ppm, 9.39 (s, 2H(2)) ppm, 7.4–7.6 (m, 15H, Ph-H) ppm; ^{13}C NMR (DMSO-d_6): 191.5 (C2), 180.8 (C4), 183.9 (C5), 188.5(C6), 185.9(C8), ^{31}P{^{1}H} NMR ($CDCl_3$): δ 29.7 (s, PPh_3).

2.3.7. Synthesis of chloro-(purine-6-thiolato)-(tris-o-tolylphosphino)palladium(II) (**6**)

(Yield: 86%). Anal. Calc. for $C_{26}H_{24}ClN_4PPdS_2$; calcd (obs): C, 46.61 (46.64); H, 3.84 (3.85); N, 8.90 (8.90); S, 10.85 (10.89). FT-IR: 1590–1637, ν(C=N), 373, ν(Pd–S), 408, ν(Pd ← N), 298, ν(Pd–Cl) cm^{-1}; ^{1}H NMR (DMSO-d_6): 6.87 (d, $^3J_{HH} = 7.2$ Hz, 1H(8)) ppm, 7.73 (d, $^3J_{HH} = 7.2$ Hz, 1H, NH(9)) ppm, 8.45 (s, 1H(2)) ppm, 7.4–7.6 (m, 12H, tolyl-H) ppm, 1.95–2.44 (m, 9H, –CH_3); ^{13}C NMR (DMSO-d_6): 189.5 (C2), 176.8 (C4), 179.9

(C5), 181.7 (C6), 178.1 (C8), $^{31}P\{^{1}H\}$ NMR ($CDCl_3$): δ 30.7 (s, (*o*-tolyl)$_3$P).

2.3.8. Synthesis of chloro-(purine-6-thiolato)(chlorodiphenylphosphino)palladium(II) (7)

(Yield: 80%). Anal. Calc. for $C_{17}H_{13}Cl_2N_4PPdS$ calcd (obs): C, 39.75 (39.75); H, 2.55 (2.50); N, 10.91 (10.91); S, 6.24 (6.25). FT-IR: 1595–1628, ν(C=N), 295, ν(Pd–Cl), 320, ν(Pd–S), 473, ν(Pd ← N) cm^{-1}; ^{1}H NMR (DMSO-d_6): 6.72 [d, $^{3}J_{HH} = 7.0$ Hz, 1H(8)] ppm, 7.96 (d, $^{3}J_{HH} = 7.0$ Hz, 1H, NH(9)) ppm, 8.23 (s, 1H(2)) ppm, 7.1–7.4 (m, 10H, Ph-H) ppm. ^{13}C NMR (DMSO-d_6): 192.3 (C2), 166.3 (C4), 160.2 (C5), 182.2 (C6), 168.24 (C8), $^{31}P\{^{1}H\}$ NMR ($CDCl_3$): δ 27.0 (s, $PClPh_2$).

2.3.9. Synthesis of chloro-(pyridine-2-thiolato)(triphenylphosphino)palladium(II) (8)

(Yield: 87%). Anal. Calc. for $C_{23}H_{19}ClNPPdS$ calcd (obs): C, 53.71 (53.75); H, 3.72 (3.70); N, 2.72 (2.71); S, 6.23 (6.23). FT-IR: 1639, ν(C=N), 295, ν(Pd–Cl), 315, ν(Pd–S), 428, ν(Pd ← N) cm^{-1}; ^{1}H NMR (DMSO-d_6): 6.72 (d, $^{3}J_{HH} = 7.0$ Hz, 1H(8)) ppm, 7.96 (d, $^{3}J_{HH} =$ 7.0 Hz, 1H, NH(9)) ppm, 7.1–7.4 (m, 15H, Ph-H) ppm. ^{13}C NMR (DMSO-d_6): 192.3 (C2), 168.24 (C3), 106.3 (C4), 108.5 (C5), 182.2 (C6), $^{31}P\{^{1}H\}$ NMR ($CDCl_3$): δ 27.0 (s, $PClPh_2$).

2.3.10. Synthesis of chloro-(pyridine-2-thiolato)-(tris(o-tolyl)phosphino)-palladium(II) (9)

(Yield: 75%). Anal. Calc. for $C_{26}H_{25}ClNPPdS$ calcd (obs): C, 56.12 (56.15); H, 4.53 (4.52); N, 2.52 (2.55); S, 5.76 (5.76). FT-IR: 1628, ν(C=N), 319, ν(Pd–Cl), 354, ν(Pd–S), 473, ν(Pd ← N) cm^{-1}, ^{1}H NMR (DMSO-d_6): 6.78 (d, $^{3}J_{HH} = 6.9$ Hz, 1H(8)) ppm, 7.86 (d, $^{3}J_{HH} =$ 6.85 Hz, 1H, NH(9)) ppm, 7.1–7.4 (m, 10H, Ph-H) ppm, 2.94 (m, 9H, –CH_3) ppm. ^{13}C NMR (DMSO-d_6): 191.3 (C2), 168.42 (C3), 105.7 (C4), 109.3 (C5), 182.9 (C6), $^{31}P\{^{1}H\}$ NMR ($CDCl_3$), δ 29.0 (s, $PClPh_2$).

2.4. Crystal structure determination

The structure of non-ionic complex **5** was determined by single-crystal X-ray diffraction. An orange crystal was selected from the reaction product and mounted with epoxy glue on a glass capillary. The measurement was carried out at 293 K using an Oxford Diffraction Xcalibur 2 diffractometer with Mo Kα radiation. The exposure time was 10 s per frame, the crystal-detector distance, 60 mm. Data reduction and analytical absorption correction were performed using the CRYSALIS RED software suite [15]. The final lattice parameters ($a = 31.6198(10)$ Å; $c =$ 18.0729(6) Å) were calculated from all reflections observed in the actual data collection. Systematic absences indicated the rhombohedral centrosymmetric space group *R-3*. The structure was solved by direct methods using SIR2004 [16], which revealed the atomic positions, and refined by using the SHELX-97 program package [17]. The final refinements were carried out on F_o^2. Atomic scattering factors for spherical neutral free atoms were taken from standard sources, and anomalous dispersion corrections were applied [18]. Difference Fourier analysis, which was performed after locating the atoms of the [Pd(Pur6S)$_2$(PPh$_3$)] molecule, showed a strong disorder for the solvent molecules. Calculations performed at an intermediate stage, in which the relative positional occupancies of the Cl positions were refined, revealed a full occupancy for Cl1 and Cl2 and partial occupancies for the remaining Cl atoms. Disorder of the solvent (0.45%) molecules was modelled using the SQUEEZE routine of the PLATON software suite [19]. Final *R* indices were $R_1 = 0.0482$, $wR_2 = 0.1315$ for $[I > 2\sigma(I)]$ and $R_1 =$ 0.0590, $wR_2 = 0.1431$ for all data.

2.5. Antifungal assay

The agar tube dilution method was used for antifungal activity assay of plant extracts with some modifications [21]. The compounds were solubilized in dimethylsulfoxide and a dilution was performed in Sabouraud dextrose agar (SDA) (Merck) medium, and acidic Media (pH 5.5–5.6) containing a relatively high concentration of glucose (40%) were prepared by mixing (SDA) and 6.5 gm/mL distilled water. The contents were dissolved and dispensed as 4 mL volumes into screw capped tubes and autoclaved at 121 °C for 20 min. Tubes were allowed to cool to 50 °C and non-solidified SDA is loaded with 67 μL of compound pipetted out from the stock solution. This gave the final concentration of 200 μg/mL of the compound in media. Tubes were then allowed to solidify in slanting position at room temperature. Tubes were prepared in triplicate for each fungus species. Other media supplemented with dimethylsulfoxide and reference antifungal drugs were used as negative and positive control respectively. Each tube was inoculated with 4 mm diameter piece of inoculums, removed from a 7 days old culture of fungus. The tubes were incubated at 28 °C for 7 days. Cultures were examined twice weekly during the incubation. The growth in the media was determined by measuring the linear growth (mm) and the growth inhibition was calculated with reference to a negative control. A growth control of the test strains and a susceptibility standard test using Terbinafine 200 μg/mL as the reference system were performed by applying the same technique.

2.6. Anti-inflammatory activity

Adult male Sprague–Dawley rats (180–230 g) were used in all the experiments. The animals were housed under optimum conditions of light and temperature (12 h light and dark cycle and 22–38 °C), with food and water provided *ad libitum*. The animals were divided into 11 groups (one control, one standard and nine test).

2.6.1. Preparation of test samples for bioassay

Test samples were suspended in 0.75% sodium carboxymethylcellulose (CMC) and were given orally to the test animals. The animals of the control group received the same experimental handling except that the drug treatment was replaced with appropriate volume of the dosing vehicle. Nine groups of three animals each received one compound i.e. 1–9 at 25 mg/kg. The standard drug Declofenac potassium 10 mg/5 mL was used as reference drug.

2.6.2. Carrageenan-induced hind paw oedema test

The rat paw oedema was induced by subcutaneous injection of 0.1% carrageenan (50 μL) into the sub plantar region of each animal left hind paw [22]. The measurement of rat paw volumes was carried out by the plythesmographic method [23]. It was done by recording the rat paw volume before the carrageenan injection at 0 h and then at 1 h intervals for 4 h. Nine groups of three animals were given 1–9 compounds (25 mg/kg), each group given one compound. The standard drug Declofenac potassium 10 mg/5 mL was used as a positive control. The negative control group received 0.75% CMC (carboxymethylcellulose) sodium. One hour later, a volume of 50 μL of carrageenan at 0.1% in distilled water was injected into the rat's peritoneal cavity. The percentage oedema inhibition was calculated for each animal group in comparison with its control treated group.

2.7. Cytotoxicity of compounds *1*, *3* and *4* against seven human tumor cell lines

The cytotoxicity of compounds **1**, **3** and **4** was tested *in vitro* by applying seven well characterized human tumor cell lines (MCF7 and EVSA-T (breast cancers), WIDR (colon cancer), IGROV (ovarian cancer), M19 MEL (melanoma), A498 (renal cancer), H226 (non-small cell lung cancer) and the microculture sulforhodamine B (SRB) test of which the protocol was described elsewhere [13,24].

Cell lines WIDR, M19 MEL, A498, IGROV and H226 belong to the currently used anticancer screening panel of the National Cancer Institute, USA.

The MCF7 cell line is estrogen receptor (ER)+/progesterone receptor (PgR)+ and the cell line EVSA-T is (ER)−/(PgR)−.

3. Results and discussion

The four-coordinate thiolate complexes of Pd(II) were isolated from the reaction mixture of $[Pd(PR_2R')_2Cl_2]$ and the corresponding heterocyclic thiolates (1:1 and 1:2 molar ratio) in dichloromethane. The isolated complexes are sketched in Scheme 1. During the synthesis the acidic proton of the ligand is abstracted by the precursor providing the anion which is trapped by the metal substrate ($PdCl_2$) moiety to form the new complex with concomitant release of HCl.

3.1. ^1H, ^{13}C and ^{31}P NMR data

The proton NMR spectra for complexes **1**–**9** shows the resonance line pattern observed for the heterocyclicthiols that has been assigned on the basis of literature data [25] (see Scheme 2).

The ^1H NMR spectra were consistent with structures with two ligands, a heterocyclic thiolate ($Pym2S^-$, $Pur6S^-$ and $Py2S^-$) and a tertiary phosphine (PPh_3, $(o\text{-tolyl})_3P$, $ClPh_2P$). In compound **1**, a doublet at 8.23 ppm (H(6), $^3J_{HH} = 7.3$ Hz) and a doublet at 6.98 ppm (H(4), $^3J_{HH} = 6.5$ Hz) are observed at room temperature. The H(6) doublet shows a downfield chemical shift as compared to the free ligand at 6.46 (d, H(3), $^3J_{HH} = 7.0$ Hz) which indicates that $Pym2S^-$ coordinates to central metal through N(1). The ring-proton H(5) of pyrimidine-2-thiolate is observed at 6.46 ppm. The considerable chemical shift differences of the $PymS^-$ ligand in these complexes with respect to the uncoordinated thiolate suggest a $pymS^-$ coordination to palladium. Almost the same chemical shifts are observed in the complexes **2** and **3**. The NH proton in all complexes shows downfield shifts whereas the other protons show an upfield shift. The resonance of the thiolate protons are downfield to TMS; these downfield shifts are in accordance with a dominant σ-delocalization pattern of spin density and are consistent with the ground state of the Pd(II) which has two unpaired electrons in σ-symmetry orbitals ($d_{x^2-y^2}$, d_{z^2}). However, the net spin density in the dπ orbitals could be polarized by the unpaired electrons in the $d_{x^2-y^2}$ and d_{z^2} orbitals via spin–orbital coupling and this mechanism can distribute spin density into the thiolate rings.

In compound **5**, the two $Pur6S^-$ ligands are in equivalent in the solid state structure. However, as described earlier, the room temperature ^1H NMR spectrum of **5** showed only one set of $Pur6S^-$ resonances. The apparent equivalence of the two $Pur6S^-$ ligands in the spectrum at room temperature can be attributed to some fluxionality in solution [26]. One set of $Pur6S^-$ acts as unidentate (S-bonded) and the other one as bidentate (N,S-bonded) and considerable downfield chemical shifts at 6.99 ppm (d, 1H(8), $^3J_{HH} = 8$ Hz), 7.23 ppm (d, 1H(9), $^3J_{HH} = 8$ Hz), 9.39 ppm (s, 1H(2)) are observed in the purine ring protons [10,27] after complexation to palladium(II). These results are also confirmed by the single crystal X-ray diffraction result. The same trend of chemical shifts in the single set

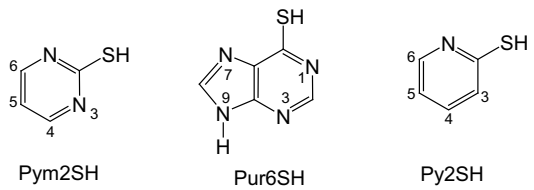

Scheme 2. Numbering scheme for the heterocyclic thiols.

of purine ring protons is observed in the compounds **4**, **6** and **7**. The absence of –SH signal is indicating a deprotonation of Pur6SH and its coordination to palladium(II) as the anionic $Pur6S^-$ moiety.

The ^1H NMR spectra of compounds **8** and **9** show a downfield chemical shift for the ring-hydrogen H(6) at 8.85 ppm (d, H(6), $^3J_{HH} = 7.4$ Hz), indicative of an N,S– mode of co-ordination of the ligand $Py2S^-$ with palladium; the H3 and H4 protons appear as a complex pattern around 7.89 ppm. The downfield shift of the proton H5 appearing at 6.43 ppm (t, 1H, pyS-H(5), $^3J_{HH} =$ 6.8 Hz) suggests that the ligands are attached to the central metal via N(1) and S in these complexes.

The ^{13}C NMR spectra of complexes exhibit low-field shifts. The N,S-chelating $Pym2S^-$ and $Pur6S^-$ moiety in the metal complexes shows low-field shifts for C(2) and C(6) carbons of the pyrimidine and purine rings [28], while the S-bonded unidentate $Pym2S^-$ exhibits a downfield shift for C(6). This is attributed to the delocalization of electron density on the pyrimidine ring [10], increasing its aromaticity relative to the free 2HPymS or N,S-chelating $Pym2S^-$ ligand. The ^{13}C NMR data of these compounds show the presence of N,S-chelating $Pym2S^-$, $Pur6S^-$, PyS^- anions, in agreement with the solid state structure results. The ^1H and ^{13}C NMR spectral data provide evidence for extensive delocalization of the charge density along the R–P–Pd–N,SR axis and the absence of any back bonding property of S atoms makes it further necessary to disperse the excess charge density received by the Pd metal centre onto the ligands. Coordination by P and N atoms lowers the energy of the *p*-orbitals of phenyl and thiolate moieties, thus enhancing their Lewis acidity.

The $^{31}P\{1H\}$ NMR spectra of the compounds run in CH_2Cl_2, relative to the external reference 85% H_3PO_4, with downfield shifts defined as positive. In complexes **1**–**9**, a single ^{31}P resonance is observed at δP, 32.85–27.00 ppm with a coordination shift (δcomplex–δligand).

3.2. Crystal structure determination

In the structure of the non-ionic complex **5** (see Fig. 1), the Pd atom is four-coordinate and exhibits a slightly distorted square-planar geometry. One of the 6-mercaptopurine molecules acts as monodentate and the other one as bidentate, the fourth coordination site of the metal cation being occupied by the triphenylphosphine. It is to be noted that, although the NMR spectra show only one set of signals for the 6-mercaptopurine ligand, corresponding to a quick fluctuation between monodentate and bidentate coordination for the molecule in solution, no disorder of the ligands was found. Both 6-mercaptopurine molecules are approximately planar, with an angle of 78.4° between the least square planes. The two chlorine atoms (Cl1 and Cl2) are coordinated via hydrogen bonds to the 6-mercaptopurine ligands, Cl2 is also connected to the PPh_3 unit of the adjacent molecule. The resulting crystal structure contains a regular arrangement of one-dimensional channels running along the *c*-axis. The walls of these channels are composed of interlocking 1D helical chains consisting of the $Pd(Pur6S)_2PPh_3$ system. The two chlorines of the 0.45 CH_2Cl_2 molecules are located in large pores (diameter: 6.8 Å), thus stabilizing the porous framework and no disorder of ligand is found in complex 5. Although the electron density of the Cl atoms of the dichloromethane unit was

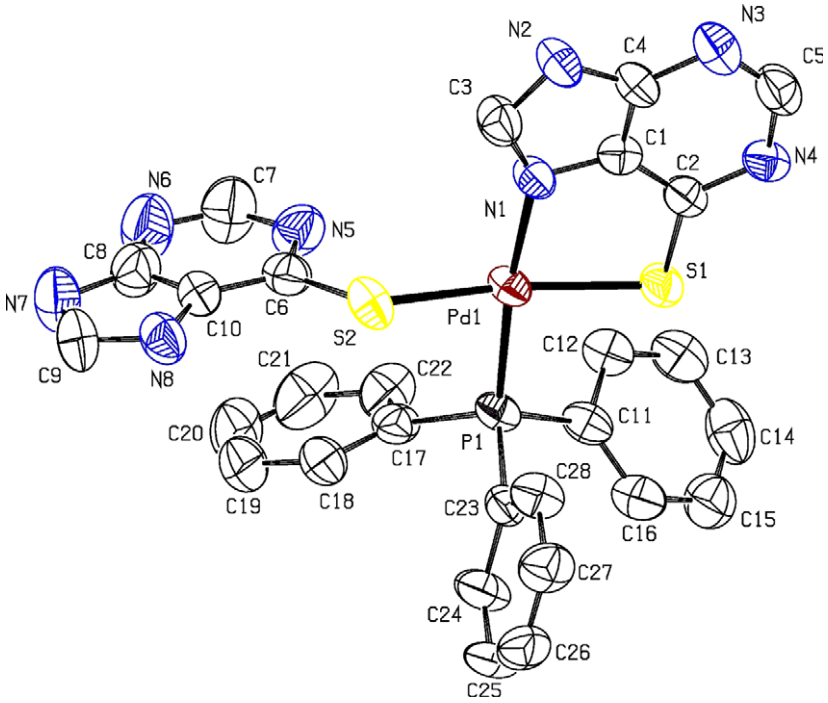

Fig. 1. ORTEP diagram of $[PdC_{28}H_{21}N_8PS_2]$ with atomic numbering scheme.

clearly visible during the refinement of the crystal structure, the central carbon atoms could not be detected. However, the distances between the chlorine atoms were in accordance with values expected for the 1,3 Cl···Cl distance in the dichloromethane molecule. The results indicate a rotational disorder of the central CH_2 unit around the Cl···Cl axis, the C/H atoms of the solvent molecules were therefore modelled using the SQUEEZE routine of the PLATON software suite [19]. The total amount of solvent was determined by refining the occupancy of the Cl atoms using fixed isotropic thermal parameters. The results suggest 8.1 dichloromethane molecules per unit cell (see Table 1).

3.3. FT-IR results

Deprotonation of the ligand is accompanied by a substantial modification of their FT-IR spectra with ν(S–H) (2600–2500 cm^{-1}) absent from the spectra of the metal derivatives **1**–**9** and a significant perturbation of the "thioamide" bands [29]. In all cases, shifts to shorter wavelengths are observed for ν(C=N) and ν(C–S) relative to the free thione, the 650 cm^{-1} band ν(C=S) is absent. Additional weak or medium intensity bands for ν(Pd–S) (≈385 cm^{-1}) as well as ν(Pd–N) (≈399–443 cm^{-1}) are observed [30,31]. Such vibrational activities and replacement of the acidic hydrogen(s) by palladium [32] are clearly indicative of a S,N-coordination [33,34] and of the formation of a four-membered chelate ring around the central metal through a donor atom set comprising the imine-nitrogen and thiolate sulfur, respectively, while a new absorption band due to ν(Pd–Cl) appears at 295–315 cm^{-1}. The observed shifts in the ligand vibrations upon coordination with respect to the free ligand are similar in all complexes. Therefore the predicted S,N-coordination of the ligand is supported by the single-crystal X-ray diffraction data. The coordination of PR_3 to the central metal atom exhibited expected results and the effect of PR_3 is also observed in some dithiocarbamate complexes [35]. The appearance of a (P–C) vibration, which occurs at 1474 cm^{-1} in PPh_3, is shifted toward 1460 cm^{-1} upon coordination. Pd–P vibration and low energy band of Pd–Cl should appear below the detection limit due to high trans influence of sulfur donor.

Table 1
Crystal data and structure refinement for complex **5**

Empirical formula	$[C_{28}H_{21}N_8PS_2Pd]$ 0.45 CH_2Cl_2
Formula weight	778.16
Temperature (K)	293(2)
Wavelength (Å)	0.7107
Crystal system	Rhombohedral
Space group	*R*-3
Unit cell dimensions	
a (Å)	31.6198(10)
c (Å)	18.0729(6)
Volume (Å^3)	15648.6(9)
Z	18
D_{calc} (Mg/m^3)	1.478
Absorption coefficient (mm^{-1})	0.876
F(000)	6953
Crystal size (mm)	0.19 × 0.11 × 0.06
Theta range for data collection (°)	4.10–20.81
Index ranges	$-31 \leqslant h \leqslant 31$, $-31 \leqslant k \leqslant 31$, $-18 \leqslant l \leqslant 18$
Reflections collected	29242
Independent reflections [R_{int}]	3609 [0.0396]
Completeness to theta = 20.81°	99.2%
Absorption correction	Analytical
Maximum and minimum transmission	0.903 and 0.791
Refinement method	Full-matrix least-squares on F^2
Data/restraints/parameters	3609/0/397
Goodness-of-fit on F^2	1.077
Final *R* indices [$I > 2\sigma(I)$]	$R_1 = 0.0477$, $wR_2 = 0.1282$
R indices (all data)	$R_1 = 0.0586$, $wR_2 = 0.1393$
Largest difference in peak and hole (e Å^{-3})	0.935 and −0.610

3.4. Antifungal activity

The results of antifungal assays showed (Table 2) that the compounds **1**–**9** possess antifungal activity against the following five fungi: *Fusarium moniliformes*, *Fusarium saolani*, *Mucor* sp., *Aspergillus niger*, *Aspergillus fumigatus*.

The rank-order of the % of inhibition effect for the fungi is *Fusarium moniliformes* > *Fusarium saolani* > *Aspergillus fumigatus* ≈ *Aspergillus niger* > *Mucor* sp. and histogram, which clearly indicated that palladium(II) complexes are significantly active against these fungi (detailed data in Table 2).

Compounds **1**, **2**, **4**, **5** and **7** at concentration of 200 μg/mL inhibited the growth of *F. moniliformes* by 78–67%. Compounds **3**, **6** and **8** showed a moderate growth inhibition of 65–52%. Comparatively compound **9** showed a lower (50%) inhibition than the other ones. The compounds **8** and **9** showed the highest activity against the *A. fumigatus* i.e. 65% and 62%, respectively. The growth inhibition of all compounds against *F. moniliformes* is

Table 2
Anti-fungal activity of palladium(II) complexes

Compounds	Growth effect %Inhibition (Fungus)				
	F. moniliformes	*F. solani*	*Mucor* sp.	*A. niger*	*A. fumigatus*
1	78.28	58	0	33.33	30.33
2	67.11	30	10	40.44	35.38
3	65.26	22	0	39.44	45.64
4	68.89	45	0	58.69	53.08
5	75.66	51	25	52.32	50.25
6	52.68	50	10	51.11	58.00
7	67.56	56	18	47.25	48.55
8	52.89	45	28	54.76	65.34
9	49.98	54	22	32.62	61.87
Linear length in −ve control	45	25	100	90	39

Terbinafine, used as control inhibited all fungi at 200 μg/mL.
−ve control group with 0.75% CMC (carboxymethylcellulose) sodium.

Table 3
Anti-inflammatory activity of palladium(II) compounds of heterocyclic thiolates on carrageenan induced rat paw oedema

Compounds	% oedema inhibition at time (h)			
	First hour	Second hour	Third hour	Fourth hour
Standard drug	2.32 ± 4.52	3.49 ± 4.32	68.70 ± 3.05	74.14 ± 2.72
1	26.74 ± 2.34	35.11 ± 4.06	45.19 ± 20.78	70.41 ± 6.35
2	18.17 ± 2.12	20.17 ± 7.72	24.42 ± 3.43	24.32 ± 1.02
3	29.84 ± 3.51	36.78 ± 6.13	69.57 ± 2.84	93.87 ± 2.35
4	22.51 ± 1.51	32.7 ± 6.13	55.33 ± 3.12	83.46 ± 3.53
5	23.84 ± 3.23	30.91 ± 5.32	68.66 ± 2.72	91.46 ± 2.25
6	18.93± 4.21	29.32 ± 3.49	73.12 ± 2.64	92.87 ± 2.34
7	25.73 ± 4.23	35.38 ± 5.32	69.47 ± 2.52	85.46 ± 2.25
8	19.54 ± 1.78	36.98 ± 2.35	76.46 ± 2.36	87.54 ± 2.14
9	18.45 ± 3.78	28.45 ± 3.65	72.65 ± 2.99	88.68 ± 1.08

Values are mean ± SEM; $n = 3$ in each group.

important, while, against *Mucor* sp., the activity of all compounds is not significant. Compounds **1**–**7** showed moderate activities against *A. niger* and *A. fumigatus* (see Fig. 2).

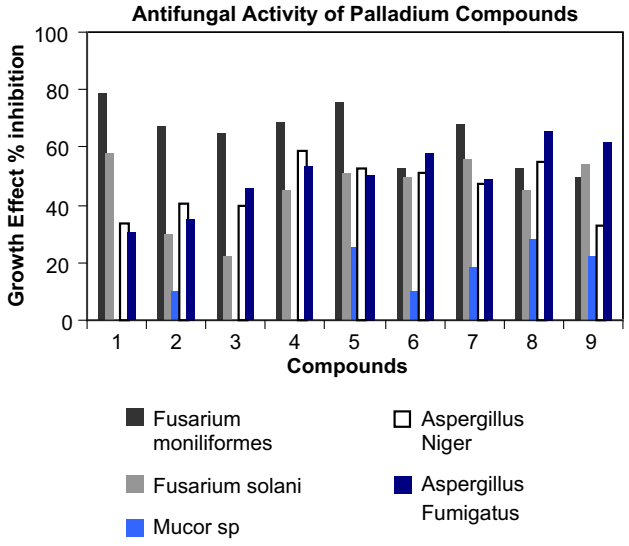

Fig. 2. Comparison of Growth% inhibition of palladium compounds against five fungi.

3.5. Anti-inflammatory activity

During the initial pharmacological evaluation of compounds **1**–**9**, it was suggested that the *in vitro* drugs' potency relative to other NSAIDs (nonsterodial anti-inflammatory drugs) produce their therapeutic activities through the inhibition of cyclooxygenase (COX), the enzyme that makes prostagladins (PGs). COX has at least two isoenzymes i.e. COX-1 which constitutes the PGs that protect the stomach and the kidney and COX-2 which induces the inflammation stimuli, such as cytokines and produces PGs that contribute to the pain and swelling of inflammation. In the present work, the anti-inflammatory action results of the synthesized compounds **1**–**9** show that the injection of carrageenan into the rat paw induces the liberation of bradykinin, which later induces the biosynthesis of prostaglandin and other autacoids (i.e. hormones that produce their physiological effect by transportation of blood) that are responsible for the formation of the inflammatory exudates [36]. From the carrageenan-induced oedema tests involving both COX-1 and COX-2 activities [37], it is not as clear whether

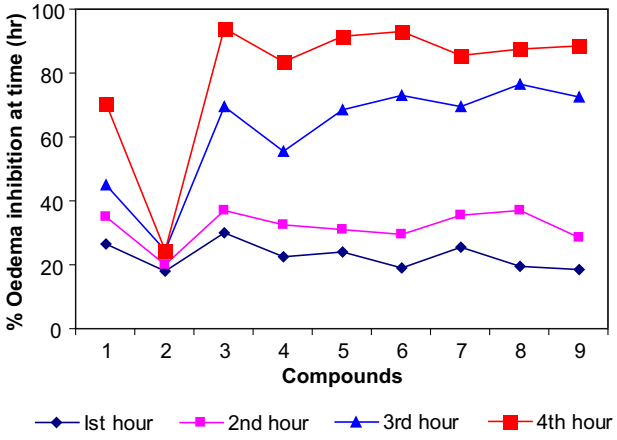

Fig. 3. Inhibition of prostaglandin biosynthesis by palladium compounds: at the 4th hour, compounds **3**, **7** and **9** showed maximum (89–93%) oedema inhibition, compounds **1**, **5**, **6** and **8** show a moderate one, compound **4** a low one and **2**, a very low inhibition, while the result of the standard drug is 74.1 ± 2.7% at the 4th hour. Three or more estimates were averaged, standard error of the mean ± SEM; $n = 3$ in each group is shown in Table 3.

Table 4
Inhibition doses ID_{50} *in vitro* cytotoxicities of compounds **1**,**3** and **4** and of six reference compounds doxorubicin (DOX), cisplatin (CPT), 5-fluorouracil (5-FU), methotrexate (MTX), etoposide (ETO) and taxol (TAX)

Compound	A498	EVSA-T	H226	IGROV	M19MEL	MCF-7	WiDr
1	2335	1097	5166	192	3382	2338	2890
3	5428	327	2756	1396	3445	1705	7033
4	12603	1561	11727	7802	6630	3212	2686
DOX	90	8	199	60	16	10	11
CPT	2253	422	3269	169	558	699	967
5FU	143	475	340	297	442	750	225
MTX	37	5	2287	7	23	18	<3
ETO	1314	317	3934	580	505	2594	150
TAX	<3	<3	<3	<3	<3	<3	<3

the complexes of palladium(II) with heterocyclic thiolates/tertiary phosphine act by inhibiting COX-1 alone or by inhibiting both COX-1 and COX-2. Therefore, it is suggested that the mechanism of action of the compounds may be related to a prostaglandin synthesis inhibition, as described for the anti-inflammatory mechanism of declofenac potassium in the inhibition of the inflammatory process induced by carrageenan [38] (see Fig. 3).

3.6. Cytotoxicity of compounds *1*, *3* and *4* against seven human tumor cell lines

Table 4 shows the experimental results.

Compounds **1** and **4** showed mostly a moderate to low cytotoxicity against the seven well characterized human tumor cell lines whereas **3** was somewhat more active.

4. Conclusion

The synthesized complexes **1**–**9** were characterized by FT-IR and multinuclear NMR spectroscopy, and single-crystal X-ray diffraction. Each technique suggests that structural changes occur in heterocyclic thiols upon deprotonation and coordination to palladium takes place through S,N– and S atoms, the other coordination positions being occupied by chloride ions and phosphorus atoms to achieve a square planar geometry around palladium. The coordination position has also been confirmed by the novel crystal structure of complex **5**, [bis(purine-6-thiolato)(triphenylphosphine)]palladium(II). The major purpose of this work was to study the structural relationship of compounds with biological systems, the study of anti-inflammatory properties to determine the relationship between N,S– and NCSS- compounds and the anti-inflammation actions (i.e. carrageenan-induced paw oedema formation). The tests were optimized by using NSAIDs (nonsteriodal anti-inflammatory drugs) Declofenac (standard drug), response was produced which blocked the oedema by 74% and the compounds shows 10–15% greater inhibition than the standard drug. However, the rank-order potency of these compounds **1**–**9** (accordingly heterocyclic thiolates) as inhibitors of COX *in vitro* is purine-6-thiolate > pyrimidine-2-thiolate > pyridine-2-thiolate. Further studies will be needed to delineate the differential effects of heterocyclic thiolate palladium(II) complexes in systems that involve both COX-1 and COX-2. At present, inhibition of COX is clearly the most likely mechanism underlying the actions of (N,S)-thiolates. This is based not only on its ability to inhibit COX *in vitro* and block prostaglandin production, but also on its inability to produce COX-independent activities. Most notably, palladium–thiolate complexes may not interact with a variety of key receptors, channels, or enzymes known to be involved in pain transmission mechanisms. Compounds **1** and **4** showed mostly a moderate to low cytotoxicity against the seven human tumor cell lines whereas compound **3** was somewhat more active.

Acknowledgement

The authors thank Professor Davide Viterbo for his crystallographic support and higher Education Commotion Islamabad, Pakistan for financial support through Project No. 20-623/R&D/06/258.

Appendix A. Supplementary material

CCDC 643263 contains the supplementary crystallographic data for compound **5**. These data can be obtained free of charge from The Cambridge Crystallographic Data Centre via www.ccdc.cam.ac.uk/data_request/cif. Supplementary data associated with this article can be found, in the online version, at doi:10.1016/j.jorganchem.2008.01.005.

References

[1] J.G. Wright, M.J. Natan, F.M. McDonnell, D.M. Ralston, T.V. O'Halloran, Prog. Inorg. Chem. 38 (1990) 323.
[2] K.C. Dash, H. SchmidbaurMetal Ions in Biological System, vol. 14, Marcel Decker, New York, 1982, p. 179.
[3] (a) P.J. Sadler, Adv. Inorg. Chem. Radiochem. 36 (1991) 1;
(b) J. Burgess, Trans. Met. Chem. 18 (1993) 439.
[4] M.J. Williams, Organic Superconductors (Including Fullerenes) Synthesis, Structure, Properties and Theory, Prentice Hall, Englewood Cliffs, NJ, 1992, p. 148.
[5] A. Mendia, E. Cerrada, F.J. Arnaiz, M. Laguna, Dalton Trans. (2006) 609.
[6] L. Serrano José, J. Pérez, Trans. Met. Chem. 27 (2002) 105.
[7] P.D. Akrivos, Coord. Chem. Rev. 213 (2001) 181.
[8] M. Das, N. Abiko, S.E. Livinstone, Brit. J. Cancer 38 (1978) 325.
[9] M. Maeda, N. Abiko, T. Sasaki, J. Med. Chem. 24 (1981) 167.
[10] P.D. Cookson, E.R.T. Tiekink, J. Chem. Soc., Dalton Trans. (1993) 259.
[11] J.A. McCleverty, N.J. Morrison, N. Spencer, C.A. Ashworth, R.C. Taylor, J. Chem. Soc., Dalton Trans. (1980) 11945.
[12] E.S. Raper, Coord. Chem. Rev. 165 (1997) 475.
[13] (a) F. Shaheen, M. Najam-Ul-Haq, A. Badshah, K. Wurst, S. Ali, Acta Crystallogr. E62 (2006) m138;
(b) F. Shaheen, A. Badshah, M. Gielen, L. Marchio, D. de Vos, M. Kaleem Khosa, Appl. Organomet. Chem. 21 (2007) 625.
[14] (a) D.D. Parrin, W.L.F. Armarego, Purification of Laboratory Chemicals, 3rd ed., Butterworth, Heenemann, Oxford, 1997, p. 573;
(b) Y. Kitanto, Y. Kinoshita, R. Nakamura, T. Ashida, Acta Crystallogr. C39 (1983) 1015.
[15] Oxford Diffraction, CRYSALIS RED v.1.71, Oxford Diffraction Ltd., Oxford, UK, 2004.
[16] M.C. Burla, R. Caliandro, M. Camalli, B. Carrozzini, G.L. Cascarano, L. De Caro, C. Giacovazzo, G. Polidori, R. Spagna, J. Appl. Crystallogr. 38 (2005) 381.
[17] G.M. Sheldrick, SHELXL-97: Program for Crystal Structure Refinement, University of Göttingen, 1997.
[18] D.T. Cromer, J.T. WaberInternational Tables for X-ray Crystallography, vol. 4, Kynoch Press, Birmingham, England, 1974, Table 2.2 A and Table 2.3.1.
[19] A.L. Spek, PLATON – A Multipurpose Crystallographic Tool, Utrecht University, 2006.
[20] D. Kovala-Demertzi, A. Domopoulou, M.A. Demertzis, G. Valle, A. Papageorgiou, J. Inorg. Biochem. 68 (1997) 147.
[21] M.I. Choudhary, Dur-e-Shahwar, Z. Parveen, A. Jabbar, I. Ali, Atta-ur-Rahman, Phytochemistry 40 (4) (1995) 1243.

[22] C.A. Winter, E.A. Risley, G.W. Nuss, Proc. Soc. Exp. Biol. Med. 111 (1962) 544.
[23] J.M. Harris, P.S.J. Spencer, J. Pharm. Pharmacol. 14 (1962) 464.
[24] (a) Y.P. Keepers, P.E. Pizao, G.J. Peters, J. van Ark-Otte, B. Winograd, H.M. Pinedo, Eur. J. Cancer 27 (1991) 897;
(b) F. Shaheen, A. Badshah, M. Gielen, C. Gieck, D. de Vos, Appl. Organomet. Chem. 21 (2007) 633;
(c) F. Shaheen, A. Badasha, M. Gielen, M. Duesk, K. Fejfarova, D. de Vos, B. Mirza, J. Organomet. Chem. 692 (2007) 3019.
[25] P.K. Baker, M.E. Harman, S. Hughes, M.B. Hursthouse, K.M. Abdul Malik, J. Org. Chem. 498 (1995) 257.
[26] A.J. Deeming, M. Karim, N.I. Powell, J. Chem. Soc., Dalton Trans. (1990) 2321.
[27] P.K. Baker, S. Hughes, J. Coord. Chem. 35 (1995) 1.
[28] J. Fornies, C. Fortuno, M.A. Gomez, B. Menjon, E. Herdtweck, Organometallics 12 (1993) 4368.
[29] G. López, G. Sánchez, G. García, J. García, A. Martínez, J.A. Hermoso, M. Martínez-Ripoll, J. Organomet. Chem. 435 (1992) 193.
[30] Y. Wang, Q. Shi, W. Bi, X. Li, R. Cao, Z. Anorg. Allg. Chem. 632 (2006) 167.
[31] G. Faraglia, S. Sitran, D. Montagner, Inorg. Chim. Acta 358 (2005) 971.
[32] L. Ronconi, C. Maccato, D. Barreca, R. Saini, M. Zancato, D. Fregona, Polyhedron 24 (2005) 521.
[33] (a) G. Faraglia, D. Fregona, S. Sitran, L. Giovagnini, C. Marzano, F. Baccichetti, U. Casellato, R. Graziani, J. Inorg. Biochem. 83 (2001) 31;
(b) A. Cavaglioni, R. Cini, J. Chem. Soc., Daltan Trans. (1997) 1149.
[34] L. Ballester, A. Gutierrez, M.F. Perfiñán, T. Rico, E. Gutierrez-Puebla, A. Monge, Polyhedron 13 (1994) 2271.
[35] N. Manav, A.K. Mishra, N.K. Kaushik, Spectrochim. Acta Part A: 60 (2004) 3087.
[36] A. Ueno, H. Naraba, Y. Ikeda, F. Ushikubi, T. Murata, S. Naramiya, S. Oh-ishi, Life Sci. 66 (2000) 155.
[37] (a) F. Nantel, D. Denis, R. Gordon, A. Northey, M. Cirino, K.M. Metters, C.C. Chan, Brit. J. Pharmacol. 128 (1999) 853;
(b) K. Seibert, Y. Zhang, K. Leahy, S. Hauser, J. Masferrer, W. Perkins, L. Lee, P. Isakson, Proc. Natl. Acad. Sci. USA 91 (1994) 12013.
[38] (a) M. Di Rosa, J.P. Giroud, D.A. Willoughby, J. Pathol. 104 (1971) 15;
(b) Y. Zhang, A. Shaffer, J. Portanova, K. Seibert, P.C. Isakson, J. Pharmacol. Exp. Ther. 283 (1997) 1069.